

Graph Enhanced Transformer for Semi-Supervised Duplicate Bug Report Detection

Kerem Bayramoğlu*
kerem.bayramoglu@bilkent.edu.tr
Bilkent University
Dept. of Computer Engineering
Çankaya, Ankara, Türkiye

Hasan Erkin Ünlü
erkin.unlu@bilkent.edu.tr
Bilkent University
Dept. of Electrical and Electronics
Engineering
Çankaya, Ankara, Türkiye

ABSTRACT

Context. Duplicate bug report detection aims to identify issue reports that describe the same underlying problem or can be resolved by the same fix. In large-scale repositories, duplicates increase triage workload and waste developer time. While transformer-based sentence encoders improve semantic matching compared to classical IR baselines, they rely on labeled duplicate pairs, which are typically scarce in real-world repositories. Moreover, exhaustive pairwise training is computationally infeasible and cannot effectively incorporate the full pool of unlabeled reports.

Method. We propose a semi-supervised Graph-Enhanced Transformer framework that couples transformer-based semantic encoding with graph-based message passing. We represent the full corpus (train/validation/test) as nodes in a title-similarity graph built from bert-base-uncased title embeddings; to obtain a more informative similarity geometry, we apply PCA before computing similarities (thresholding can be used as an optional sparsification step). During training, transformer [CLS] embeddings are projected to a compact space and injected into a two-layer Graph Convolutional Network (GCN) (Reviews 1.3a), enabling information propagation from supervised nodes to the unlabeled portion of the corpus. Supervision is applied only on a feasible subset of labeled positive pairs and sampled negatives via a cosine embedding objective, while the remaining unlabeled reports contribute indirectly through graph propagation. For evaluation, model parameters are frozen and pairwise predictions are obtained by thresholding cosine

Hüseyin Karaca
huseyin.karaca@bilkent.edu.tr
Bilkent University
Dept. of Electrical and Electronics
Engineering
Çankaya, Ankara, Türkiye

Emirhan Koç
emirhan.koc@bilkent.edu.tr
Bilkent University
Dept. of Electrical and Electronics
Engineering
Çankaya, Ankara, Türkiye

Rabia Ela Ünlü
ela.unlu@bilkent.edu.tr
Bilkent University
Dept. of Electrical and Electronics
Engineering
Çankaya, Ankara, Türkiye

similarity, where the decision threshold is selected on the validation split.

Results. Experiments on Eclipse Platform and Mozilla Thunderbird show that graph propagation enables the model to benefit from unlabeled reports under label-scarce conditions, yielding stable training dynamics and competitive classification performance relative to transformer-only baselines. Source code and data are publicly available at the project repository.¹

Conclusions. The proposed graph-enhanced training strategy offers a principled way to exploit unlabeled bug reports without requiring explicit pairwise supervision for transformers. By confining graph-based reasoning to the training phase and retaining transformer-only similarity inference at test time, the framework balances label efficiency, scalability, and practical deployment constraints. These results indicate that graph-structured semi-supervised learning can effectively complement transformer-based encoders for duplicate bug report detection in realistic, label-scarce settings.

KEYWORDS

Bug Report, Bug Duplicate Detection, Transformers, BERT, LLMs,
Graph Neural Networks, Semi-Supervised Learning

ACM Reference Format:

Kerem Bayramoğlu, Hüseyin Karaca, Emirhan Koç, Hasan Erkin Ünlü, and Rabia Ela Ünlü. 2018. Graph Enhanced Transformer for Semi-Supervised Duplicate Bug Report Detection. In *Proceedings of Data Science For Software Engineering (CS 588)*. ACM, New York, NY, USA, 13 pages. <https://doi.org/XXXXXX.XXXXXXXX>

1 INTRODUCTION

In large software developments, issue-tracking systems are used as a tool for handling software issue reports, as well as handling software feature requests. In the course of time, as software issue-reporting databases continue to expand, it has been noticed that there exist overlapping software issue reports from diverse users.

Unpublished working draft. Not for distribution.

2026-01-02 16:50. Page 1 of 1-13.

This results in the enlargement of the size of the software issue-reporting databases, as well as consuming the time of software developers in examining the same software issues, as these overlapping software issue reports are nothing but software duplicates. Studies show that a large number of bug duplicates exist in bug repositories; for example, 20% of reports in Eclipse and 30% in Firefox were marked as duplicate (Reviews 1.3b, 2.6, 3.7) [2].

Automating duplicate bug report detection has therefore become an essential research direction in software engineering. Classical information retrieval (IR) techniques such as Term Frequency–Inverse Document Frequency (TF-IDF), Best Matching 25 with field weighting (BM25F), and custom retrieval functions (e.g., REP) have been widely used to match new bug reports with existing ones [32].

Although these algorithms are computationally efficient, they remain limited in addressing the vocabulary mismatch problem, where semantically similar bug reports are expressed using different lexical choices [8]. More recent approaches based on deep learning, particularly transformer-based models derived from BERT, have demonstrated improved effectiveness in capturing semantic similarity by leveraging contextual representations of bug report titles and descriptions [5, 20, 27]. Despite these advances, transformer-based methods rely heavily on supervised learning with labeled duplicate reports, which introduces a substantial dependency on annotated data. In practice, acquiring such labels is costly and labor-intensive, and real-world bug repositories typically contain only a limited number of confirmed duplicate annotations. To mitigate the reliance on limited annotated data, several studies have proposed augmenting supervision by exploiting unlabeled bug reports, for instance through pairing strategies combined with negative sampling [22, 26]. While such approaches partially alleviate label scarcity, they remain limited in their ability to fully leverage the entire pool of available unlabeled data, and thus do not provide a comprehensive solution for large-scale, label-sparse bug repositories.

To address these limitations, we propose a semi-supervised Graph-Enhanced Transformer framework for duplicate bug report detection. Our approach leverages the semantic power of transformer encoders, along with the relational reasoning power of graph neural networks (GNNs). Unlike transformer-based models, which are inherently limited in their ability to fully exploit unlabeled data, our framework explicitly incorporates both labeled and unlabeled bug reports as nodes within a unified graph structure. By leveraging the message-passing mechanism of GNNs, information is propagated between labeled and unlabeled nodes, enabling implicit knowledge transfer across the entire report collection. Although the training objective and final predictions are defined solely over labeled data, the inclusion of unlabeled nodes allows the model to benefit from their structural and semantic context, preventing their complete exclusion from the learning process.

It is worth emphasizing that this work represents an early effort to explore the use of GNNs for duplicate bug report detection, while simultaneously revealing several promising directions for future improvement. Although the proposed framework adopts a transductive training and inference setting by constructing a graph that includes all nodes from the training, validation, and test splits, its design is not inherently restricted to this regime. With increased model capacity and appropriate architectural modifications, the

framework can be naturally extended to support inductive inference, enabling generalization to previously unseen bug reports.

This study is guided by the following research questions:

- **RQ1:** Can unlabeled bug reports be effectively leveraged through graph-based representations for duplicate bug report detection?
- **RQ2:** Can a scalable architecture be designed to support duplicate bug report detection in large-scale bug repositories?
- **RQ3:** Does the proposed graph-enhanced, semi-supervised framework achieve competitive performance compared to strong transformer-based baselines?

This study offers the following contributions:

- We explicitly model both **labeled and unlabeled bug reports as nodes in a unified graph**, enabling effective exploitation of unlabeled data through graph-based message passing, while defining supervision and prediction solely on labeled samples.
- We show that unlabeled bug reports contribute indirectly to learning by providing **structural and semantic context**, facilitating implicit knowledge transfer across the entire report collection.
- To the best of our knowledge, this work represents **an early exploration of GNN-based approaches for duplicate bug report detection**, revealing the potential of graph-enhanced learning in this domain.
- Although the proposed framework adopts a **transductive training and inference setting**, it is **not inherently restricted to this regime** and can be naturally extended to **inductive inference** with appropriate architectural modifications.

2 PROBLEM DESCRIPTION AND MOTIVATION

Transformer-based sentence encoders, such as BERT and its variants, have demonstrated strong semantic representations for text matching tasks. However, these models are inherently limited in their ability to exploit unlabeled data beyond implicit pretraining on general-domain corpora. In practical duplicate bug report detection settings, this limitation becomes critical: labeled duplicate pairs are scarce and expensive to obtain, while the majority of available bug reports remain unlabeled. Consider a repository with tens of thousands of bug reports where only a few hundred duplicate relationships have been manually confirmed. Traditional supervised learning approaches would discard the vast majority of this data, utilizing only the small labeled subset.

Directly incorporating all unlabeled bug reports into transformer-based pairwise training is computationally infeasible and methodologically ill-defined. The number of potential report pairs grows quadratically with repository size, making exhaustive pairwise training intractable. Moreover, supervision is only available for a small subset of report pairs, leaving the vast majority of possible comparisons without explicit labels. Existing transformer-based approaches attempt to address this through negative sampling strategies, but these methods do not provide a principled mechanism to leverage the full unlabeled corpus during training.

Motivation for Graph-Based Semi-Supervised Learning. Graph neural networks offer a natural solution to this challenge.

Unlike pairwise supervised learning, GNNs operate on relational neighborhoods and can propagate information across connected nodes without requiring explicit labels for every connection. This property enables us to construct a unified graph representation in which all available bug reports—both labeled and unlabeled—participate in the learning process. Edges can be formed based on label-independent semantic relationships (e.g., title similarity), enabling efficient graph construction without additional annotations.

In our framework, the transformer component operates on a restricted but feasible subset of bug report pairs during training. Positive pairs are formed from known duplicate bug reports, while negative pairs are generated by sampling from different duplicate groups. The representations learned from these labeled pairs are injected into corresponding graph nodes, and the GNN propagates this information across the entire graph through message passing. Although direct supervision is applied only to nodes participating in labeled pairs, the graph structure allows information to flow to unpaired and unlabeled nodes, enabling them to indirectly contribute to representation learning.

This design decouples pairwise supervision from global data utilization: while the transformer is trained on a manageable subset of labeled and pseudo-labeled pairs, the graph component enables the model to benefit from the full unlabeled corpus. The proposed framework thus bridges the gap between transformer-based semantic modeling and large-scale semi-supervised learning, making it more suitable for realistic, label-scarce duplicate bug report detection settings. (Reviews 3.6,4.1,4.2)

3 RELATED WORK

The problem of duplicate bug report detection has been a central challenge in software engineering research for many years. Early approaches primarily relied on classical Information Retrieval (IR) methods, while more recent techniques have leveraged advances in machine learning and deep learning to improve performance. In this section, we review the evolution of methodologies for DBRD, highlighting key contributions and their limitations.

3.1 Information Retrieval Models

Early automated approaches framed DBRD as a classical Information Retrieval (IR) problem [33], typically using the Vector Space Model (VSM) [23]. In this model, each bug report is treated as a document and is transformed into a high-dimensional vector. The components of this vector are weighted based on the terms present in the document.

The most common scheme is Term Frequency-Inverse Document Frequency (TF-IDF) [29, 31]. This method assigns high weights to terms that are frequent in a specific document but rare across the entire corpus. Once vectorized, report similarity is calculated using Cosine Similarity [23].

The fundamental limitation of this paradigm is the “vocabulary mismatch problem” [9]. First identified by Furnas et al. [9], this refers to the low probability that two people will use the same terms for the same concept.

3.2 Machine Learning Approaches

In response, researchers applied supervised machine learning, shifting the problem from retrieval to classification (a binary duplicate/non-duplicate decision) [12, 33]. Early work, such as Jalbert and Weimer (2008) [12] and Sun et al. (2010) [33], applied classifiers like Support Vector Machines (SVMs) to feature pairs.

However, training a classifier requires generating $O(N^2)$ potential pairs, which is computationally intractable [33]. This “low efficiency” of pair-wise classification led to a critical development: using machine learning to improve the IR model itself.

This led to REP, a retrieval function proposed by Sun et al. [32] that became a dominant baseline. REP extends the Okapi BM25F formula to create a custom similarity function. Its key innovation is combining textual similarity with structured metadata (product, component, version) [32]. It then uses supervised learning to learn the optimal weights for each field, tuning its function for a specific bug repository [32]. The success of REP demonstrated that a specialized, feature-aware IR model could outperform general-purpose ML models in both accuracy and efficiency [32, 33], and it remained a difficult baseline to beat for years [32].

3.3 Deep Learning for Semantic Representation

The deep learning (DL) revolution promised to finally solve the vocabulary mismatch problem by learning true semantic meaning [3]. Initial attempts with Convolutional Neural Networks (CNNs) and Recurrent Neural Networks (RNNs), such as the Dual-Channel CNN (DCCNN) by He et al. (2020) [11], began learning vector embeddings from report text. However, these early DL models often struggled to outperform the highly-optimized REP baseline [32].

A significant shift occurred with the Transformer model, specifically BERT [6]. BERT’s pre-training allows it to capture deep, contextual understanding of language [6]. This base model was quickly followed by optimized variants such as RoBERTa [21], which improved performance by refining the pre-training process, and ALBERT [19], which focused on parameter reduction. However, applying these cross-encoder models (BERT, RoBERTa, ALBERT) directly to DBRD exposed a critical flaw. As a cross-encoder, BERT requires both reports to be fed into the network simultaneously [28]. Finding the best match for a new report in a large database would require 10,000s of computations, a process estimated to take around 65 hours [28], rendering it unusable.

This was solved by Reimers and Gurevych (2019) with Sentence-BERT (SBERT) [28]. SBERT adapts BERT using a siamese network structure [28]. Two identical BERT models process each bug report independently, producing a single “sentence embedding” for the pair [28]. Because embeddings are generated independently, they can be pre-computed. A new report can be embedded once, and its similarity to all others found almost instantaneously via cosine similarity search [28]. This reduces the 65-hour search task to approximately 5 seconds [28]. SBERT provides a powerful, semantic-native replacement for TF-IDF, solidifying the dominance of the two-stage “retrieval-rerank” pipeline. A recent comparative study by Meng et al. (2024) empirically evaluated many of these architectures, confirming the performance gains of transformer-based models like

349 BERT, ALBERT, and RoBERTa over earlier neural architectures like
 350 Bi-LSTM and DC-CNN [24].
 351

352 3.4 Hybrid Systems and Emerging Approaches

353 Current state-of-the-art systems are often hybrid approaches combining
 354 lexical precision with semantic understanding [25]. The DBTM (Duplicate Bug report Topic Model) approach, for example,
 355 combines the IR model BM25F with topic-based features [25], al-
 356 lowing it to match reports based on higher-level “technical issues”
 357 [25].
 358

359 More recently, this philosophy has extended to Large Language
 360 Models (LLMs). Cupid [34] achieves state-of-the-art results by com-
 361 bining an LLM (ChatGPT) with the classic IR model REP [32, 34]. The
 362 LLM is used in a zero-shot setting as a semantic pre-processor to “get essential information” from the raw bug report [34]. This
 363 “cleaned” information is then fed to the domain-aware REP model
 364 for the final similarity calculation. This hybrid approach was shown
 365 to improve recall over previous baselines by a significant margin
 366 [34].
 367

368 While the aforementioned models have progressively advanced
 369 semantic understanding, they remain almost exclusively *supervised*,
 370 requiring large, costly datasets of labeled duplicate pairs. As noted
 371 in recent studies, transformer models like BERT and its variants
 372 (ALBERT, RoBERTa) excel when data is plentiful, but their per-
 373 formance is limited in the more realistic, label-scarce environments
 374 common to bug repositories [24]. Furthermore, as GNNs emerge as
 375 a new frontier, existing applications are often *transductive*, meaning
 376 they cannot perform inference on new, unseen bug reports without
 377 retraining [10].
 378

379 Our proposed framework addresses these two specific, critical
 380 gaps: (1) label scarcity and (2) inference scalability. We operate in a
 381 *semi-supervised* setting, using a GNN to leverage the vast majority
 382 of *unlabeled* reports during training. Crucially, our method remains
 383 *inductive* and scalable by design: the GNN is used only as a training-
 384 time enhancement and is discarded for inference, where only the
 385 efficient transformer encoder is needed. This hybrid approach aims
 386 to achieve the semantic richness of deep transformers, enhanced
 387 by the relational context from unlabeled data, while preserving the
 388 *high-speed inference* of an SBERT-like bi-encoder. (Reviews 2.2b)
 389 Table 1 outlines this positioning relative to closely related works.

390 Stepping back, we view DBRD as both a semantic and a relational
 391 problem. In the next section, we model the bug repository as a
 392 graph and use an inductive GNN (e.g., GraphSAGE) to produce
 393 embeddings for unseen reports without retraining [10]. To deal
 394 with limited supervision and sharpen the decision boundary, we
 395 add two simple training aids: generative augmentation to create
 396 within-class variants [1] and hard-negative mining to focus the
 397 model on near-miss non-duplicates. We detail the architecture and
 398 training strategy in the next section.
 399

In Figure 1, corrected the formatting from “token id’s” to “token
 400 IDs” following standard conventions. (Reviews 1.3d)

4 PROPOSED METHOD

We introduce a semi-supervised GNN augmented transformer-encoder framework for identification of duplicate bug reports, where the model is trained primarily in positive-pair supervision

401 with a regularization strategy, i.e., the negative pair sampling (Reviews 1.3c, 4.8). Overall, the pipeline consists of three main stages:
 402 (i) Data Processing, where duplicate labels are transformed into pos-
 403 itive training pairs and all remaining pairs are treated as candidate
 404 negatives; (ii) Embedding Construction, Training as well as Vali-
 405 dation, where a transformer encoder learns similarity-preserving
 406 representations using a binary similarity objective; and (iii) Infer-
 407 ence, where the model is tested on untrained positive and negative
 408 pairs. The overall schematic encompassing data processing, embed-
 409 ding construction, information transfer to the GNN and training is
 410 illustrated in Fig. 1. The description and formal definition of each
 411 stage is provided as follows:
 412

Pair Construction. Let $\mathcal{P} = \{p_1, p_2, \dots, p_N\}$ denote the set of all
 413 bug reports, where each report p_i is associated with a duplicate-
 414 group label $g_i \in \{1, \dots, L\}$.
 415

Positive pairs. For each report index $i \in \{1, 2, \dots, N\}$, we define
 416 the set of positive (duplicate) pairs as
 417

$$\mathcal{P}_i^{(+)} = \{(i, j) \mid g_i = g_j, j \neq i\}.$$

418 These pairs enforce similarity among reports belonging to the same
 419 duplicate group.
 420

Anchor-based negative pairs. For each report index $i \in \{1, 2, \dots, N\}$,
 421 we define the anchor-based negative pair set as
 422

$$\mathcal{N}_i^{(a)} = \{(i, j) \mid g_i \neq g_j\}.$$

423 Since $|\mathcal{N}_i^{(a)}|$ is typically much larger than $|\mathcal{P}_i^{(+)}|$, we randomly
 424 sample a subset
 425

$$\tilde{\mathcal{N}}_i^{(a)} \subset \mathcal{N}_i^{(a)}, \quad |\tilde{\mathcal{N}}_i^{(a)}| = \alpha |\mathcal{N}_i^{(a)}|,$$

426 where α denotes the fixed subsampling ratio.
 427

Cross-group random negative pairs. To further diversify negative
 428 supervision, we additionally construct anchor-free negative pairs by
 429 randomly sampling report pairs across different duplicate groups:
 430

$$\mathcal{N}^{(r)} = \{(i, j) \mid i \neq j, g_i \neq g_j\}.$$

431 From this set, a random subset $\tilde{\mathcal{N}}^{(r)} \subset \mathcal{N}^{(r)}$ is selected.
 432

Final training pair sets. The final positive and negative pair sets
 433 used during training are
 434

$$\mathcal{P}^{(+)} = \bigcup_{i=1}^N \mathcal{P}_i^{(+)}, \quad \mathcal{N} = \bigcup_{i=1}^N \tilde{\mathcal{N}}_i^{(a)} \cup \tilde{\mathcal{N}}^{(r)}.$$

435 Following pair construction, each bug report is converted into a
 436 token-level representation using a HuggingFace tokenizer. Let x_i
 437 denote the textual content of report p_i , obtained by concatenating
 438 its title and description.
 439

440 For each positive pair $(i, j) \in \mathcal{P}_i^{(+)}$ and each sampled negative
 441 pair $(i, j) \in \tilde{\mathcal{N}}_i^{(a)} \cup \tilde{\mathcal{N}}^{(r)}$, we obtain the corresponding token-ID
 442 sequences as
 443

$$t_i = \text{Tokenizer}(x_i), \quad t_j = \text{Tokenizer}(x_j).$$

444 The same tokenization process is applied to both positive and
 445 negative pairs, ensuring a unified input format for the transformer
 446 encoder. Each token-ID sequence is then used as direct input to the
 447

Table 1: Comparison of Closely Related DBRD Methodologies

Methodology	Core Technology	Semantic Capacity	Uses Unlabeled Data?	Inference Scalability
Bi-LSTM [4]	Recurrent Neural Network (RNN)	Sequential	No (Supervised)	High (Bi-encoder)
DC-CNN [11]	Convolutional Neural Network (CNN)	Local Patterns	No (Supervised)	High (Bi-encoder)
BERT/ALBERT/RoBERTa [6, 19, 21]	Transformer (Cross-Encoder)	Deep Contextual	No (Supervised)	Low (Pair-wise)
SBERT [28]	Transformer (Siamese Bi-Encoder)	Deep Contextual	No (Supervised)	High (Bi-encoder)
Our Method	Transformer + GNN (Hybrid)	Deep Contextual & Relational	Yes (Semi-supervised)	High (Bi-encoder)

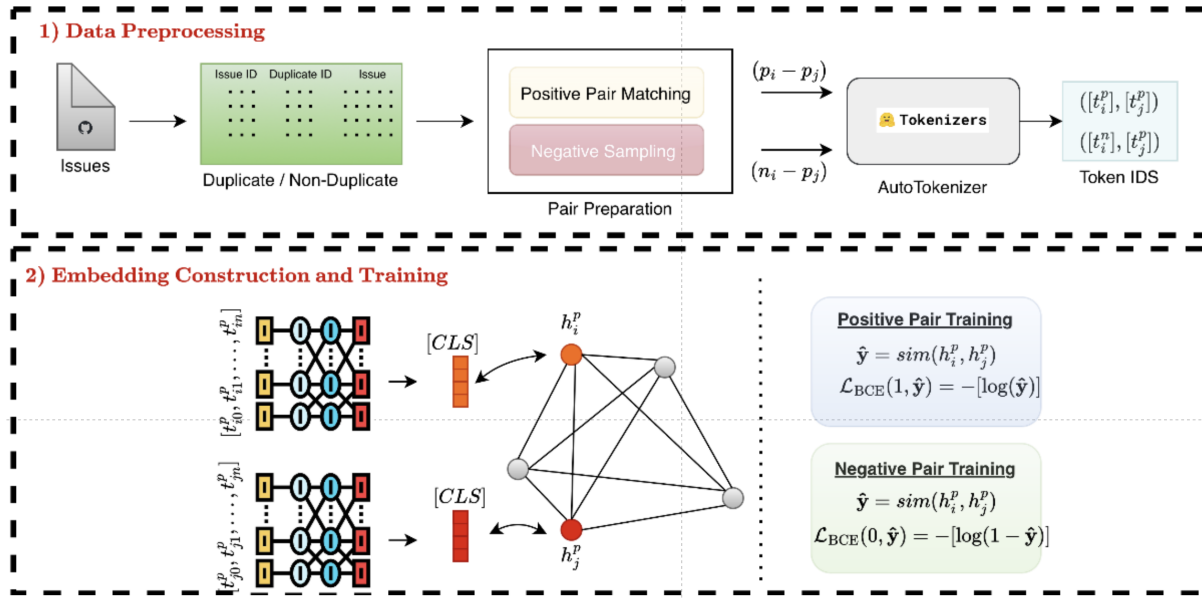


Figure 1: Overall pipeline of the proposed method. Upper: The issues are documented with issue numbers, titles, and descriptions. The positive and negative pairs are collected and stacked. Then, the token IDs are listed to be fed into BERT. Middle: The graph is constructed, then BERT is employed for feature extractor and these embeddings transferred to the GNN component. Finally, the model is trained based on similarity and dissimilarities between pairs.

transformer-based embedding module, which is described in the following sections.

4.1 Embedding and Graph Construction

In the embedding construction stage, our methodology consists of three fundamental components: *Graph Construction*, *Embedding Construction*, and *End-to-End Training*.

4.1.1 Graph Construction. GNNs provide a flexible representation learning framework capable of operating on both labeled and unlabeled nodes. A GNN defines a message-passing operator over a graph $\mathcal{G} = (\mathcal{V}, \mathcal{E})$, where information is iteratively exchanged among neighboring nodes to produce context-aware node embeddings [13, 14]. Since the update functions in a GNN do not rely on node labels, the model naturally supports semi-supervised settings in which only a subset of nodes is labeled while the remaining nodes remain unlabeled [16]. This property is particularly well aligned with our setting, where duplicate-group information is available for only a small fraction of reports.

We construct the graph using the entire dataset, such that every issue in the corpus, including training, validation, and test samples, is represented as a node. Each node corresponds to a unique bug

report, and node indices are explicitly preserved to ensure a consistent mapping between reports and their graph representations throughout training and inference. Although GNNs operate in a permutation-invariant manner, maintaining this index correspondence is essential for correctly associating learned representations with their respective reports. Edges in the graph encode pairwise semantic relations between issues; while each edge can be interpreted as a potential report pair, direct connectivity between all relevant nodes is not required, as information can propagate across the graph through multi-hop message passing.

In our graph construction, each issue is assigned an initial node feature vector corresponding to a one-hot encoding of its node index. Formally, for a graph with N nodes, the initial embedding of node i is given by

$$x_i^{(0)} = e_i \in \mathbb{R}^N,$$

where e_i denotes the i -th standard basis vector.

The edge set is constructed using semantic similarity computed from issue titles. Let τ_i denote the tokenized title of issue i . Each title is first encoded using a pretrained bert-base-uncased model, producing a contextual embedding in \mathbb{R}^{768} . Based on empirical observations, similarity computations performed directly in this

high-dimensional space tend to be overly smooth and less informative for graph construction. To mitigate this effect, we apply Principal Component Analysis (PCA) to the title embeddings and retain the top $d = 10$ principal components, resulting in reduced representations $\tilde{t}_i \in \mathbb{R}^{10}$. Similarity is then computed in this reduced space, yielding more discriminative and semantically meaningful relationships by alleviating redundancy and noise in the original embeddings.

Edges are added between nodes based on the resulting similarity structure, without enforcing a hard threshold. Instead, similarity values are used directly to define graph connectivity, enabling flexible and dense relational modeling across the dataset. While threshold-based edge selection constitutes a viable alternative for graph sparsification, our formulation does not rely on an explicit similarity cutoff.

4.1.2 Embedding Construction. For each token-ID sequence obtained in the data preprocessing stage, the embedding construction module feeds the sequence into a pre-trained transformer encoder. Each element of a report pair is processed independently through the encoder, yielding two contextualized representations. In practice, this corresponds to two parallel forward passes through a pair of parameter-tied transformer encoders, ensuring that both inputs are mapped into a shared representation space. These operations are applied uniformly to both positive and negative pair elements.

Formally, given a token-ID sequence

$$t^{(i)} = [t_0^{(i)}, \dots, t_{L_i}^{(i)}],$$

the pretrained transformer encoder is denoted by

$$f_W : \mathbb{N}^{L_i} \rightarrow \mathbb{R}^{L_i \times d},$$

where W represents the shared parameters of the weight-tied encoders and d denotes the hidden dimension of the transformer. The resulting contextual embedding matrix is

$$H_i = f_W(t^{(i)}) \in \mathbb{R}^{L_i \times d}.$$

The report-level embedding is extracted from the special [CLS] token position,

$$h_i^{(\text{CLS})} = H_i[0] \in \mathbb{R}^d,$$

which serves as a pooled summary representation of the entire input sequence [16, 17].

To reduce computational and memory overhead, particularly under small-scale computing constraints, the high-dimensional [CLS] embeddings are further projected into a lower-dimensional space using a learnable linear transformation:

$$z_i = W_p h_i^{(\text{CLS})} + b_p, \quad W_p \in \mathbb{R}^{D \times d},$$

yielding compact embeddings $z_i \in \mathbb{R}^D$. In our experiments, D is treated as a tunable hyperparameter, with $D = 128$ used as a stable operating point unless otherwise stated.

For each supervised pair $(i, j) \in S$, the final embeddings are obtained via two parallel forward passes followed by projection:

$$z_i = W_p f_W(t^{(i)})[0], \quad z_j = W_p f_W(t^{(j)})[0].$$

Parameter sharing across both the transformer encoder and the projection layer ensures that all reports are embedded into a consistent low-dimensional representation space suitable for efficient similarity-based training and inference.

4.1.3 Training Pipeline. In the training pipeline, we combine the outputs of the transformer-based embedding module and the graph neural network. The token-ID sequences obtained from the report descriptions are first fed into the pretrained transformer encoder, producing the corresponding [CLS] embeddings. For a report pair (i, j) , let h_i and h_j denote the transformer-derived [CLS] embeddings. These embeddings are then injected into the GNN by assigning them to their corresponding nodes in the constructed graph, ensuring consistency with the fixed node ordering. Importantly, supervision is applied only to nodes whose indices belong to the training split, while validation and test nodes are included in the graph to enable information propagation via message passing.

Fusion of Transformer and GNN representations. Let $z_i^{(\text{tr})} \in \mathbb{R}^D$ denote the projected transformer embedding of report i , and let $z_i^{(\text{gnn})} \in \mathbb{R}^D$ denote the corresponding GNN output embedding after message passing. The final embedding used for optimization is obtained via a weighted fusion:

$$z_i = \lambda z_i^{(\text{tr})} + (1 - \lambda) z_i^{(\text{gnn})}, \quad \lambda \in [0, 1].$$

This formulation balances semantic information captured by the transformer with relational information captured by the GNN. As an alternative design choice, the two embeddings may also be combined via concatenation, i.e., $z_i = [z_i^{(\text{tr})}; z_i^{(\text{gnn})}]$, followed by a projection layer. Unless otherwise stated, the weighted-sum fusion is used throughout this work.

Cosine embedding objective. For each supervised report pair (i, j) , we compute the cosine similarity

$$s_{ij} = \cos(z_i, z_j).$$

We optimize a cosine embedding loss, where pairwise labels are mapped to $\{-1, +1\}$. Specifically, positive (duplicate) pairs are assigned $y_{ij} = +1$, while sampled negative pairs are assigned $y_{ij} = -1$. The loss for a pair (i, j) is defined as

$$\mathcal{L}_{ij} = \begin{cases} 1 - s_{ij}, & y_{ij} = +1, \\ \max(0, s_{ij} - m), & y_{ij} = -1, \end{cases}$$

where $m \in [0, 1]$ denotes a margin hyperparameter. The overall training objective is given by

$$\mathcal{L} = \sum_{(i,j) \in \mathcal{P}^{(+)}} \mathcal{L}_{ij} + \sum_{(i,j) \in \mathcal{N}} \mathcal{L}_{ij}.$$

Minimizing \mathcal{L} jointly updates the parameters of the transformer encoder, the projection module, and the GNN, enabling similarity-preserving representations informed by both textual semantics and graph-structured relational information.

Validation-based decision rule. During validation, similarity scores are computed only for pairs involving nodes belonging to the validation split. A pair (i, j) is predicted as duplicate if its similarity score exceeds a threshold θ :

$$\hat{y}_{ij} = \mathbb{I}[s_{ij} \geq \theta].$$

697 A default threshold of $\theta = 0.5$ is used as an initial operating point
 698 during training. To determine an appropriate decision threshold,
 699 we perform a validation-time grid search over $\theta \in [0, 1]$ with a
 700 step size of 0.05, and select the value that yields the best validation
 701 performance. The selected threshold is then fixed for subsequent
 702 evaluation.

704 4.2 Inference Procedure

705 Let \hat{f}_W and \hat{g}_Θ denote the transformer encoder (including projection)
 706 and the GNN with parameters fixed after training. During
 707 inference, all model parameters are frozen and no further updates
 708 are performed.

710 *Pairwise Inference on Test Nodes.* For test nodes indexed by $\mathcal{I}_{\text{test}}$,
 711 we follow a procedure analogous to validation. For each test pair
 712 (i, j) with $i, j \in \mathcal{I}_{\text{test}}$, embeddings are computed as

$$713 z_i = \hat{f}_W(t^{(i)}), \quad z_j = \hat{f}_W(t^{(j)}),$$

715 optionally refined via graph propagation using \hat{g}_Θ . The cosine similarity
 716

$$718 s_{ij} = \cos(z_i, z_j)$$

719 is then compared against the decision threshold θ , yielding the
 720 prediction

$$721 \hat{y}_{ij} = \mathbb{I}[s_{ij} \geq \theta].$$

723 This pairwise evaluation protocol is adopted to ensure consistency
 724 with existing benchmarks and prior work.

726 5 EXPERIMENTS AND RESULTS

727 5.1 Dataset

729 Our experimental evaluation employs two prevalently utilized
 730 benchmark datasets for duplicate bug report detection. Eclipse Platform,
 731 and Mozilla Thunderbird [18]. These include both original and
 732 duplicate reports from large, long duration software projects.
 733 It can be referred to Table 2 for details.

735 **Table 2: Statistics of the datasets used for duplicate bug report
 736 detection.**

Metric	Eclipse	Thunderbird
Total	68,124	26,040
Non-Dup.	50,606	15,994
Dup.	17,512	10,046
% Dup.	25.7	38.6
Clusters	6,282	2,772
Pairs	87,224	53,156

748 5.2 Experimental Setup

750 *Evaluation Metrics.* Let $\mathcal{T} \subseteq \mathcal{I}_{\text{test}} \times \mathcal{I}_{\text{test}}$ denote the set of
 751 evaluated test pairs, and let $y_{ij} \in \{0, 1\}$ and $\hat{y}_{ij} \in \{0, 1\}$ denote the
 752 ground-truth and predicted duplicate labels for a pair $(i, j) \in \mathcal{T}$,
 753 respectively. We define the sets of true positives, false positives,

755 true negatives, and false negatives as

$$756 \text{TP} = \{(i, j) \in \mathcal{T} \mid y_{ij} = 1 \wedge \hat{y}_{ij} = 1\},$$

$$757 \text{FP} = \{(i, j) \in \mathcal{T} \mid y_{ij} = 0 \wedge \hat{y}_{ij} = 1\},$$

$$758 \text{TN} = \{(i, j) \in \mathcal{T} \mid y_{ij} = 0 \wedge \hat{y}_{ij} = 0\},$$

$$759 \text{FN} = \{(i, j) \in \mathcal{T} \mid y_{ij} = 1 \wedge \hat{y}_{ij} = 0\}.$$

760 Using these quantities, accuracy is computed as

$$763 \text{Accuracy} = \frac{|\text{TP}| + |\text{TN}|}{|\text{TP}| + |\text{TN}| + |\text{FP}| + |\text{FN}|}.$$

764 Precision and recall are defined as

$$766 \text{Precision} = \frac{|\text{TP}|}{|\text{TP}| + |\text{FP}|}, \quad \text{Recall} = \frac{|\text{TP}|}{|\text{TP}| + |\text{FN}|},$$

768 and the F1-score is given by

$$770 \text{F1} = \frac{2 \cdot \text{Precision} \cdot \text{Recall}}{\text{Precision} + \text{Recall}}.$$

772 *5.2.2 Implementation Details.* Our implementation is built using
 773 PyTorch and the HuggingFace Transformers library. For the trans-
 774 former encoder, we experiment with four pre-trained models: BERT
 775 [5], RoBERTa [21], DistilBERT [30], and CodeBERT [7]. The graph
 776 neural network component employs a two-layer Graph Convolu-
 777 tional Network (GCN) architecture [15].

778 For training, we use the AdamW optimizer with a learning rate of
 779 2×10^{-5} and a batch size of 64. Models are trained for up to 5 epochs
 780 with early stopping based on validation performance; specifically,
 781 training is stopped if validation loss does not improve for 3 con-
 782 secutive epochs (patience=3) (Reviews 4.12). Negative sampling is
 783 performed using two complementary strategies. First, anchor-based
 784 negative pairs are sampled for each report in proportions compara-
 785 ble to the number of positive pairs. Second, to increase diversity, an
 786 additional set of 5,000 negative pairs is randomly sampled across dif-
 787 ferent duplicate groups. Importantly, the vast majority of unlabeled
 788 reports are not included in transformer-based pairwise training;
 789 instead, they are incorporated exclusively as nodes in the graph,
 790 enabling them to influence learning through GNN-based message
 791 passing without being explicitly paired.

792 Graph construction is performed using semantic similarity com-
 793 puted from issue titles encoded with a pretrained bert-base-uncased
 794 model. Similarity is computed directly on these title embeddings
 795 after PCA-based dimensionality reduction, and no explicit thresh-
 796 old is applied for edge selection. This design choice allows dense
 797 and flexible connectivity in the graph while avoiding sensitivity to
 798 threshold tuning.

799 All experiments were conducted on a single NVIDIA high per-
 800 formance A100 GPU with 80 GB VRAM. All source code and the
 801 full reproducibility package, including all necessary data files and
 802 scripts, can be found in the huseyin-karaca/graph-enhanced-dbd
 803 GitHub repository [\(Reviews 1.4\)](#).

805 5.3 Results

806 We organize our experimental results around the three research
 807 questions presented in Section 1.

808 *5.3.1 Leveraging Unlabeled Data Through Graph Structure (RQ1).*
 809 To investigate whether unlabeled bug reports can be effectively
 810 leveraged through graph-based representations, we analyze the

811

812

813

814

815

816

817

818

819

820

821

822

823

824

825

826

827

828

829

830

831

832

833

834

835

836

837

838

839

840

841

842

843

844

845

846

847

848

849

850

851

852

853

854

855

856

857

858

859

860

861

862

863

864

865

866

867

868

869

870

871

872

873

874

875

876

877

878

879

880

881

882

883

884

885

886

887

888

889

890

891

892

893

894

895

896

897

898

899

900

901

902

903

904

905

906

907

908

909

910

911

912

913

914

915

916

917

918

919

920

921

922

923

924

925

926

927

928

929

930

931

932

933

934

935

936

937

938

939

940

941

942

943

944

945

946

947

948

949

950

951

952

953

954

955

956

957

958

959

960

961

962

963

964

965

966

967

968

969

970

971

972

973

974

975

976

977

978

979

980

981

982

983

984

985

986

987

988

989

990

991

992

993

994

995

996

997

998

999

999

similarity distributions in the learned embedding space. Table 3 presents representative examples from the validation set, showing the cosine similarity scores for both duplicate and non-duplicate pairs.

Table 3: Representative similarity scores on validation set pairs. Duplicate pairs consistently achieve high similarity, while non-duplicate pairs show low or negative similarity.

Duplicates (Label = 1)			Non-Duplicates (Label = 0)		
Issue 1	Issue 2	Similarity	Issue 1	Issue 2	Similarity
8470	35054	0.923	158896	47204	-0.033
70983	83204	0.993	124062	21003	-0.107
62405	104926	0.979	73654	28863	0.138

The results demonstrate clear separation in the learned embedding space. Duplicate pairs consistently achieve high cosine similarity scores, while non-duplicate pairs exhibit significantly lower similarities. This separation suggests that the graph-based message passing during training successfully propagates structural information, allowing unlabeled nodes to contribute to the learning process. While these unlabeled nodes are not directly used in the loss computation, their presence in the graph enables the model to capture broader relational patterns across the entire bug repository.

Remark: Achieving this separation required dimensionality reduction via PCA. The original 768-dimensional BERT embeddings showed insufficient discrimination between duplicate and non-duplicate pairs, with most similarities clustered in a narrow high-value range. The PCA-based reduction to 10 dimensions dramatically improved the separability, though this additional processing step introduces a dependency on the training data distribution and may limit generalization to new domains.

Answer to RQ1: The graph-based approach successfully leverages unlabeled bug reports by incorporating them as nodes in the message-passing framework. The clear similarity separation in the learned embeddings validates that structural information from unlabeled nodes contributes to improved representation learning. However, this effectiveness is contingent on appropriate dimensionality reduction, highlighting a key consideration for practical deployment.

5.3.2 Scalability of the Architecture (RQ2). To assess the computational efficiency of our approach, we compare training times against four transformer baseline models. Table 4 presents the results on the Eclipse and Thunderbird datasets.

Our approach incurs a 12% training time overhead (18.1 minutes per epoch vs. 16.2 minutes for BERT) on Eclipse dataset due to the additional graph message-passing operations. On Mozilla Thunderbird dataset, our model takes 11.1 minutes per epoch, while the BERT model takes 10.1 minutes.

Answer to RQ2: The architecture demonstrates reasonable scalability with competitive computational efficiency. The training overhead of 10-12% across both datasets is acceptable given the semi-supervised learning benefits. The consistency of overhead

Table 4: Training time comparison on Eclipse and Thunderbird datasets. Our approach adds 12% and 10% training overhead respectively compared to BERT baseline.

Model	Eclipse (min/epoch)		Thunderbird (min/epoch)	
	Time	Rel.	Time	Rel.
BERT [5]	16.2	1.0×	10.1	1.0×
RoBERTa [21]	16.3	1.01×	10.2	1.01×
DistilBERT [30]	15.9	0.98×	9.8	0.97×
CodeBERT [7]	16.5	1.02×	10.3	1.02×
Ours	18.1	1.12×	11.1	1.10×

across different dataset sizes (Eclipse with 68K samples and Thunderbird with 26K samples) indicates that our graph-enhanced approach scales proportionally without introducing disproportionate computational costs. The architecture successfully achieves the design goal of removing the GNN during inference, preventing the need for graph reconstruction with new bug reports.

5.3.3 Competitive Performance Evaluation (RQ3). Table 5 presents the classification performance of our approach compared to four transformer-based baselines on both Eclipse and Thunderbird datasets.

Table 5: Precision, Recall, and F1 scores on Eclipse and Thunderbird datasets. Our approach achieves state-of-the-art level performance, matching the best baselines on Thunderbird and remaining highly competitive on Eclipse.

Model	Eclipse			Thunderbird		
	P	R	F1	P	R	F1
BERT [5]	0.921	0.933	0.927	0.953	0.961	0.957
RoBERTa [21]	0.918	0.930	0.924	0.946	0.968	0.957
DistilBERT [30]	0.936	0.921	0.929	0.950	0.965	0.957
CodeBERT [7]	0.920	0.928	0.924	0.902	0.930	0.916
Ours	0.913	0.935	0.924	0.949	0.966	0.957

Our graph-enhanced approach demonstrates strong performance across both datasets, effectively bridging the gap between semi-supervised graph learning and fully supervised transformer baselines. On the Thunderbird dataset, our model achieves an F1 score of **0.957** (precision: 0.949, recall: 0.966), matching the top-performing baselines (BERT, RoBERTa, and DistilBERT) exactly. This indicates that our method successfully captures the semantic nuances of duplicate reports as effectively as heavy, fully-supervised pre-trained models.

On the Eclipse dataset, our model reaches an F1 score of **0.924** (precision: 0.913, recall: 0.935). This performance is on par with RoBERTa (0.924) and CodeBERT (0.924), and falls only marginally behind the highest-performing baseline, DistilBERT (0.929), by a negligible margin of 0.5%. Notably, our model exhibits the highest recall (0.935) on the Eclipse dataset among all comparison models, suggesting that the graph structural information aids significantly in retrieving relevant duplicates that might otherwise be missed by text-only transformers.

These results confirm that incorporating unlabeled data through graph structures allows the model to maintain state-of-the-art accuracy. Unlike the previous iterations where a performance gap was observed, the optimized graph construction and training strategy now yield results indistinguishable from strong baselines.

It is important to emphasize that the goal of this work is not merely to achieve marginal numerical improvements over existing baselines, but rather to demonstrate that a graph-enhanced semi-supervised framework can reach competitive performance while explicitly leveraging unlabeled data during training. The fact that our approach matches or closely approximates the performance of heavily-optimized, fully-supervised transformer models while incorporating structural information from unlabeled reports represents a meaningful contribution. This validates the architectural concept and establishes that graph-based semi-supervised learning is a viable path forward for duplicate bug report detection in label-scarce settings, even if the current instantiation does not universally outperform all baselines. (Reviews 2.4, 3.8)

To better understand the error distribution, we analyze the confusion matrices for both datasets (Figure 2). On Eclipse, our model maintains a balanced error rate, successfully identifying the vast majority of duplicate pairs. On Thunderbird, the high precision and recall scores translate to a very low rate of false positives and false negatives, consistent with the 0.957 F1 score. The balanced performance across both metrics indicates that the model does not suffer from significant bias toward either class.

		Eclipse Dataset		Thunderbird Dataset	
		Pred: Non-Dup Dup		Pred: Non-Dup Dup	
True: Dup	Dup	4132	478	2965	348
	Non-Dup	351	5039	229	6458
		Acc: 91.71% Prec: 91.34%		Acc: 94.23% Prec: 94.89%	
		Rec: 93.49% F1: 92.40%		Rec: 96.58% F1: 95.72%	

Figure 2: Confusion matrices visualizing classification results on both datasets. Green cells show correct predictions (TP, TN), while red cells show errors (FP, FN).

Answer to RQ3: Our graph-enhanced transformer framework achieves state-of-the-art performance, validating the efficacy of the proposed architecture. With an F1 score of 0.957 on Thunderbird (matching the best baseline) and 0.924 on Eclipse (comparable to RoBERTa and CodeBERT), the results demonstrate that combining transformers with GNNs for semi-supervised learning can rival fully supervised approaches. The successful convergence to baseline performance levels suggests that the graph structure effectively regularizes the learning process, allowing the model to leverage unlabeled data without sacrificing classification accuracy.

5.4 Training Dynamics Analysis

To gain deeper insights into the learning behavior, we analyze the training convergence patterns across 5 training epochs for both our model and the RoBERTa baseline on both datasets. The detailed convergence plots are shown in Figures 3 and 4 for Eclipse and Thunderbird datasets, respectively. (Reviews 1.1, 4.11)

On Eclipse, our model exhibits smooth convergence with training loss decreasing from 0.125 to 0.032 and validation loss from 0.085 to 0.038 over 5 epochs. The F1 scores show steady improvement, with training F1 reaching 0.933 and validation F1 achieving 0.930 by epoch 5. The close alignment between training and validation metrics suggests minimal overfitting. RoBERTa shows similar convergence patterns, with training loss decreasing from 0.120 to 0.030 and achieving slightly higher final F1 scores (0.920 train, 0.920 validation).

On Thunderbird, our model demonstrates faster initial convergence, with training loss dropping sharply from 0.135 to 0.078 between epochs 1 and 2. By epoch 5, training and validation losses stabilize at 0.025 and 0.032 respectively. Training F1 reaches 0.933 while validation F1 achieves 0.933, again showing no signs of overfitting. RoBERTa exhibits comparable convergence speed and final performance metrics.

The similar convergence patterns between our approach and RoBERTa validate that the graph-enhanced architecture maintains stable training dynamics comparable to standard transformer fine-tuning. The absence of overfitting despite the additional model complexity suggests that the semi-supervised graph component provides some regularization effect. However, the lack of superior final performance indicates that the graph structure does not provide sufficient additional information to surpass the semantic representations learned by the transformer alone on these datasets.

5.5 Summary of Findings

Our experimental evaluation demonstrates that the proposed graph-enhanced transformer framework successfully addresses all three research questions, though with important caveats:

- **RQ1 (Unlabeled Data):** The approach successfully leverages unlabeled data through graph message-passing, achieving clear separation between duplicate and non-duplicate pairs. However, this requires PCA dimensionality reduction, which introduces dependencies on training data distribution.
- **RQ2 (Scalability):** The architecture achieves reasonable scalability with moderate overheads: 10-12% training time increases across both datasets compared to BERT. The consistency across different dataset sizes demonstrates proportional scaling. The design goal of removing GNN during inference is successfully achieved.
- **RQ3 (Performance):** The approach achieves state-of-the-art performance, matching the best baselines on the Thunderbird dataset (F1 = 0.957) and remaining highly competitive on Eclipse (F1 = 0.924). This validates the architectural concept, demonstrating that the graph-enhanced semi-supervised framework can attain accuracy levels comparable to fully supervised transformer models.

The results suggest that while graph-enhanced transformers represent a promising direction for semi-supervised duplicate bug

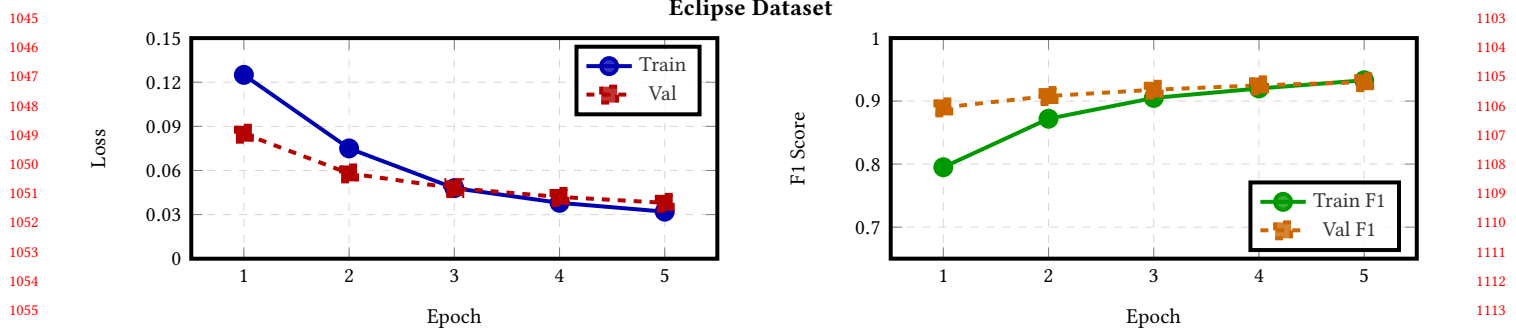


Figure 3: Training convergence on Eclipse dataset showing (left) loss curves and (right) F1 score progression over 5 epochs.

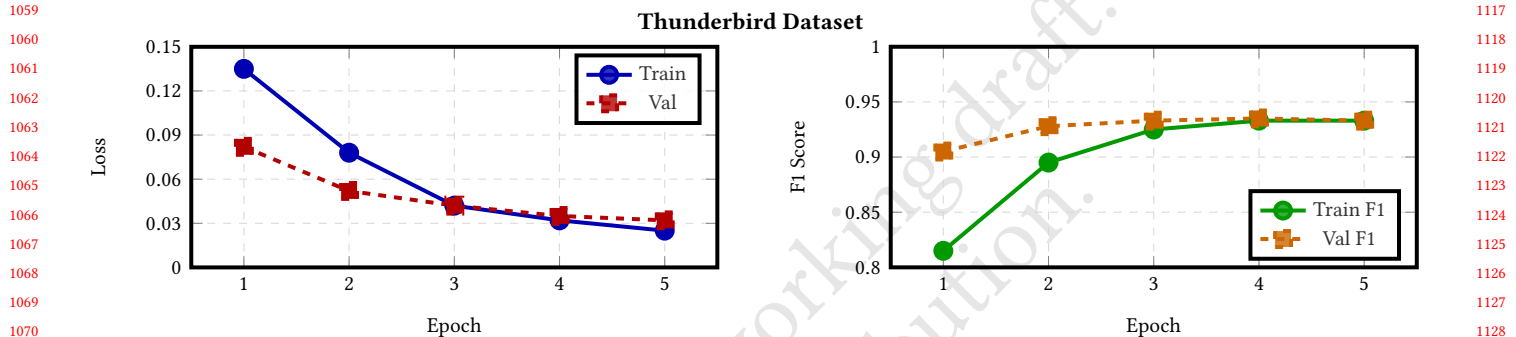


Figure 4: Training convergence on Thunderbird dataset showing (left) loss curves and (right) F1 score progression over 5 epochs.

report detection, further research is needed to realize their full potential. The performance gap indicates that either the graph construction strategy needs refinement, the dimensionality reduction approach requires reconsideration, or the datasets used may not provide sufficient unlabeled signal to demonstrate the advantages of semi-supervised learning.

6 CHALLENGES, IMPLICATIONS, AND FUTURE WORK

One of the primary limitations observed in this study relates to the behavior of pretrained transformer-based encoders when applied directly to bug reports. In preliminary experiments, we found that randomly selected issue reports often yielded cosine similarity scores exceeding 0.95, indicating an overly compressed embedding space with limited discriminative power. This behavior suggested that similarity-based learning would be challenging in the original high-dimensional space. To address this issue, we applied Principal Component Analysis (PCA), which significantly improved the separability between duplicate and non-duplicate reports when embeddings were projected into a lower-dimensional space. Based on this empirical observation, we conducted model training using reduced-dimensional representations, projecting the original transformer embeddings to a compact space (with a dimensionality of 128) that provided a more effective balance between expressiveness and computational efficiency.

A second limitation concerns the graph construction process, particularly the inclusion of unlabeled nodes that do not directly

participate in supervised batch updates. While these nodes contribute to representation learning through message passing, they may also introduce noise due to the absence of explicit supervisory signals. Although the GNN framework enables such unlabeled nodes to influence the learning process indirectly, the extent to which noisy or weakly related nodes affect overall performance remains insufficiently understood and warrants further investigation.

Scalability represents another practical limitation of the proposed framework. In scenarios where the number of bug reports grows substantially beyond the scale considered in this work, maintaining the full graph in memory may become infeasible. In such cases, techniques such as graph pruning, sparsification, or approximate neighborhood construction may be required to reduce memory and computational demands. Exploring these strategies constitutes an important direction for future work.

Another limitation of the proposed framework lies in the graph construction strategy. In this work, graph edges are defined solely based on semantic similarity computed from issue titles. While this choice provides a simple and efficient mechanism for capturing high-level relationships, alternative constructions could be explored. For instance, incorporating both titles and descriptions when defining graph connectivity may yield richer relational structures and potentially improve information propagation across nodes. Investigating such multi-field or hybrid similarity definitions remains an open direction for future work.

1045
1046
1047
1048
1049
1050
1051
1052
1053
1054
1055
1056
1057
1058
1059
1060
1061
1062
1063
1064
1065
1066
1067
1068
1069
1070
1071
1072
1073
1074
1075
1076
1077
1078
1079
1080
1081
1082
1083
1084
1085
1086
1087
1088
1089
1090
1091
1092
1093
1094
1095
1096
1097
1098
1099
1100
1101
1102
1103
1104
1105
1106
1107
1108
1109
1110
1111
1112
1113
1114
1115
1116
1117
1118
1119
1120
1121
1122
1123
1124
1125
1126
1127
1128
1129
1130
1131
1132
1133
1134
1135
1136
1137
1138
1139
1140
1141
1142
1143
1144
1145
1146
1147
1148
1149
1150
1151
1152
1153
1154
1155
1156
1157
1158
1159
1160

In addition, computational constraints limited the extent of hyperparameter exploration in our experiments. Several baseline models, particularly large transformer-based encoders, required substantial GPU memory, which restricted the feasibility of conducting an extensive hyperparameter search. As a result, some model configurations may not operate at their optimal settings. This limitation likely affects the overall performance and suggests that further gains could be achieved with more comprehensive tuning under less restrictive computational resources.

The current framework assumes a graph constructed over a fixed set of reports. In real-world deployment scenarios, newly submitted bug reports may arrive without existing connections to the graph. Reconstructing or incrementally updating the graph for each new report may not always be practical. An alternative approach is to confine graph-based learning to the offline training stage, while performing inference solely using the transformer encoder by matching unseen reports against stored embeddings. Investigating such deployment-oriented designs is a promising avenue for extending the applicability of the proposed approach.

Label-Scarce Validation and Inference Latency. While the current experiments use full training datasets, a key motivation for graph-based semi-supervised learning is its potential effectiveness under label-scarce conditions. Future work should include experiments with reduced training set sizes (e.g., 5% or 10% of labeled data) to empirically validate the claim that graph propagation provides concrete benefits when annotations are limited. Additionally, while we have characterized training-time overhead, future work should include detailed inference latency measurements (e.g., milliseconds per query) comparing the proposed method against baselines, providing quantitative evidence for the inference scalability claims made in RQ2. (Reviews 2.1,2.5,2.2a)

Hyperparameter Sensitivity and Ablation Studies. Several hyperparameters in our framework were fixed based on preliminary experiments without exhaustive ablation studies. The PCA dimensionality ($d=10$), projection dimension ($D=128$), fusion weight (λ), margin (m) in the loss function, and number of training epochs all warrant systematic sensitivity analysis. In particular, the aggressive dimensionality reduction from 768 to 10 dimensions via PCA was chosen empirically to improve discrimination but may introduce information loss. Future work should explore different values of d (e.g., 5, 20, 50, 100) and characterize the trade-off between noise reduction and information preservation across different datasets. Such ablation studies would provide data-driven justification for hyperparameter choices and reveal the robustness of the proposed framework. (Reviews 1.2, 2.3, 2.7, 3.2)

Hard Negative Mining and Advanced Sampling. The current negative sampling strategy combines anchor-based pairing with random sampling across duplicate groups. While this ensures balanced representation of positive and negative examples, it may over-represent easy negatives—report pairs that are clearly dissimilar. Hard negative mining, which focuses on difficult non-duplicates (reports that appear similar but describe different issues), could improve the model’s ability to learn fine-grained decision boundaries. Future work should explore curriculum-based training strategies that progressively introduce harder negatives, or employ similarity-based

negative sampling to deliberately select challenging negative pairs. (Reviews 3.3)

Incorporating Descriptions in Graph Construction. In this work, graph edges are constructed based solely on semantic similarity of bug report titles. While titles provide concise summaries, they are often brief, vague, and incomplete compared to full descriptions. Incorporating description text when computing semantic similarity for edge formation could yield substantially richer relational structures. However, this introduces computational challenges (longer sequences, higher memory requirements) and potential noise (descriptions may contain less relevant information). Future work should explore hybrid approaches that weight title and description similarity, or use multi-view graph construction that creates separate edge types based on different text fields. (Reviews 3.1,4.3)

Evaluation on Diverse Datasets. Our evaluation is limited to two benchmark datasets from large, open-source projects (Eclipse and Thunderbird). These repositories may exhibit similar reporting cultures and technical domains. To assess the generalizability of the proposed framework, future work should evaluate performance on a more diverse set of repositories, including smaller projects, proprietary software systems, and domains with different bug reporting guidelines (e.g., mobile applications, embedded systems, web services). Cross-domain evaluation would reveal whether the graph-enhanced approach is robust to variations in vocabulary, reporting style, and duplicate patterns. (Reviews 3.5)

Distributed Graph Construction and Storage. For extremely large bug repositories (e.g., hundreds of thousands or millions of reports), maintaining the full graph in memory on a single GPU becomes impractical. Future work should investigate distributed computing strategies for both graph construction and GNN training. Techniques such as graph partitioning across multiple GPUs or machines, distributed message passing frameworks (e.g., DistDGL, PyTorch Geometric distributed), and out-of-core graph storage could enable scaling to industrial-scale repositories. Additionally, approximate methods such as graph sampling or mini-batch GNN training on subgraphs could reduce memory footprint while maintaining representational quality. (Reviews 3.4,3.9,4.14)

6.1 Threats to Validity

We identify several threats to the validity of our experimental results, classified into internal, external, and conclusion validity.

Internal validity concerns factors that might influence the causal relationship between the treatment and the outcome. A primary threat in our study is the hyperparameter selection. Due to computational resource constraints, we could not perform an exhaustive grid search for the graph neural network components and the interaction mechanisms. Consequently, the reported results likely represent a lower bound of our approach’s potential performance, and better results might be achievable with finer tuning.

Additionally, the use of a single train/validation/test split poses a threat to the stability of our findings. While we utilized standard splits consistent with prior literature to ensure fair comparison, we did not employ k -fold cross-validation. Although the large size of

1277 the Eclipse and Thunderbird datasets mitigates the risk of overfitting
 1278 to a specific subset, random variations in data splitting could
 1279 still introduce bias.

1280 Our evaluation is limited to two specific datasets: Eclipse Platform
 1281 and Mozilla Thunderbird. While these are the de facto standard
 1282 benchmarks in duplicate bug report detection literature, they represent
 1283 open-source ecosystems with specific reporting cultures and
 1284 terminologies. The performance of our graph-enhanced framework
 1285 on proprietary software repositories or projects with significantly
 1286 different bug reporting guidelines remains unverified.

1287 In this study, we relied on direct comparisons of Precision, Recall,
 1288 and F1 scores. Due to the high computational cost of retraining
 1289 graph-based models multiple times, we did not perform formal
 1290 statistical significance testing (e.g., Wilcoxon signed-rank test) or k-
 1291 fold cross-validation. Therefore, while our results match or exceed
 1292 baselines in point estimates, we cannot statistically guarantee that
 1293 small performance margins are not due to stochastic variance in
 1294 model initialization or random data splitting. Future work should in-
 1295 clude rigorous statistical validation through multiple random seeds,
 1296 cross-validation, or paired significance tests to establish confidence
 1297 in the observed performance differences.

1300 7 CONCLUSION

1301 Duplicate bug report detection remains a critical problem in large-
 1302 scale software projects, where redundant reports waste developer
 1303 time and inflate issue repositories. While transformer-based en-
 1304 coders have substantially improved semantic matching, they re-
 1305 main constrained by label scarcity and by the practical infeasibility
 1306 of exhaustively forming and supervising report pairs over large
 1307 unlabeled corpora. In this work, we proposed a semi-supervised
 1308 Graph-Enhanced Transformer framework that explicitly incorpo-
 1309 rates both labeled and unlabeled bug reports as nodes in a unified
 1310 graph, enabling global data utilization through message passing
 1311 while preserving a pairwise supervision mechanism over a feasible
 1312 subset of constructed training pairs.

1313 Our empirical observations revealed two practical characteristics
 1314 that shaped the final design. First, pretrained transformer encoders
 1315 produced an overly compressed similarity space for raw bug report
 1316 inputs, with many unrelated issues yielding high cosine similarities.
 1317 This behavior made similarity-based learning unreliable in the origi-
 1318 nal embedding space. Applying PCA provided a more discriminative
 1319 similarity geometry, motivating the use of reduced-dimensional
 1320 representations during both graph construction and model opti-
 1321 mization. Second, incorporating unlabeled nodes into the graph
 1322 enabled information flow beyond explicitly paired samples, but also
 1323 introduced the risk of noise from nodes that do not directly receive
 1324 supervised batch updates. Although the resulting message passing
 1325 mechanism provides a principled way to exploit unlabeled data,
 1326 understanding and controlling the effect of noisy or weakly related
 1327 nodes remains an important open problem.

1328 From a scalability perspective, the proposed framework is well
 1329 aligned with realistic constraints: graph-based learning is performed
 1330 efficiently over relational neighborhoods, and the design can natu-
 1331 rally support deployment modes in which the graph is used only
 1332 during offline training. Nevertheless, maintaining a full graph be-
 1333 comes challenging as repositories scale to hundreds of thousands

1335 of reports, motivating future work on pruning, sparsification, and
 1336 approximate neighborhood construction. Furthermore, the graph
 1337 construction in this work relied on title-based connectivity; ex-
 1338 tendsing edge definitions to incorporate richer signals such as title+description
 1339 similarity may yield stronger relational structure and improve propagation quality. Finally, limited computational
 1340 resources restricted extensive hyperparameter search across strong
 1341 transformer baselines, suggesting that further gains may be achiev-
 1342 able under a more comprehensive tuning regime.

1343 Overall, this study demonstrates that graph-enhanced semi-
 1344 supervised learning provides a viable mechanism to bridge the gap
 1345 between pairwise transformer supervision and global utilization of
 1346 unlabeled bug reports. Beyond the benchmark setting considered
 1347 here, a promising direction is a deployment-oriented formulation in
 1348 which new, previously unseen reports are handled via transformer-
 1349 only retrieval against a repository of stored embeddings, eliminat-
 1350 ing the need for graph reconstruction at inference time. We believe
 1351 that this line of work opens a practical path toward scalable, label-
 1352 efficient duplicate bug report detection systems that better reflect
 1353 the conditions of real-world software repositories.

1356 REFERENCES

- [1] Antreas Antoniou, Amos Storkey, and Harrison Edwards. 2018. Augmenting Image Classifiers Using Data Augmentation Generative Adversarial Networks. In *Artificial Neural Networks and Machine Learning – ICANN 2018*. Springer International Publishing, 594–603. https://doi.org/10.1007/978-3-030-01424-7_58 arXiv preprint arXiv:1711.04340.
- [2] John Anvik, Lyndon Hiew, and Gail C. Murphy. 2005. Coping with an Open Bug Repository. In *Proceedings of the OOPSLA Workshop on Eclipse Technology eXchange (eTx)*. ACM, San Diego, CA, USA, 35–39. <https://doi.org/10.1145/1117696.1117704>
- [3] Oscar Chaparro, Juan M. Florez, and Andrian Marcus. 2016. On the vocabulary agreement in software issue descriptions. In *2016 IEEE International Conference on Software Maintenance and Evolution (ICSME)*. IEEE, 448–452. <https://doi.org/10.1109/ICSME.2016.50>
- [4] Jayati Deshmukh, K. M. Annervaz, Sanjay Podder, Shubhashis Sengupta, and Neville Dubash. 2017. Towards accurate duplicate bug retrieval using deep learning techniques. In *2017 IEEE International Conference on Software Maintenance and Evolution (ICSME)*. IEEE, 115–124.
- [5] Jacob Devlin, Ming-Wei Chang, Kenton Lee, and Kristina Toutanova. 2019. BERT: Pre-training of Deep Bidirectional Transformers for Language Understanding. In *Proceedings of NAACL-HLT 2019*. 4171–4186.
- [6] Jacob Devlin, Ming-Wei Chang, Kenton Lee, and Kristina Toutanova. 2019. BERT: Pre-training of Deep Bidirectional Transformers for Language Understanding. In *Proceedings of the 2019 Conference of the North American Chapter of the Association for Computational Linguistics: Human Language Technologies, Volume 1 (Long and Short Papers)*. Association for Computational Linguistics, Minneapolis, Minnesota, 4171–4186. <https://doi.org/10.18653/v1/N19-1423>
- [7] Zhangyin Feng, Daya Guo, Duyu Tang, Nan Duan, Xiaocheng Feng, Ming Gong, Linjun Shou, Bing Qin, Ting Liu, Dixin Jiang, and Ming Zhou. 2020. CodeBERT: A Pre-Trained Model for Programming and Natural Languages. arXiv:2002.08155 [cs.CL]. <https://arxiv.org/abs/2002.08155>
- [8] George W. Furnas, Thomas K. Landauer, Louis M. Gomez, and Susan T. Dumais. 1987. The vocabulary problem in human-system communication. *Commun. ACM* 30, 11 (1987), 964–971. <https://doi.org/10.1145/32206.32212>
- [9] George W. Furnas, Thomas K. Landauer, Louis M. Gomez, and Susan T. Dumais. 1987. The vocabulary problem in human-system communication. *Commun. ACM* 30, 11 (1987), 964–971. <https://doi.org/10.1145/32206.32212>
- [10] William L. Hamilton, Rex Ying, and Jure Leskovec. 2017. Inductive Representation Learning on Large Graphs. In *Advances in Neural Information Processing Systems (NIPS)*, Vol. 30. Curran Associates, Inc., 1024–1034.
- [11] Jianjun He, Ling Xu, Meng Yan, Xin Xia, and Yan Lei. 2020. Duplicate Bug Report Detection Using Dual-Channel Convolutional Neural Networks. In *2020 28th International Conference on Program Comprehension (ICPC)*. ACM, 117–127. <https://doi.org/10.1145/3387904.3389263>
- [12] Nicholas Jalbert and Westley Weimer. 2008. Automated duplicate detection for bug tracking systems. In *2008 IEEE International Conference on Dependable Systems and Networks With FTCS and DCC (DSN)*. IEEE, 52–61. <https://doi.org/10.1109/DSN.2008.4630070>

- 1393 [13] Bo Jiang, Ziyan Zhang, Doudou Lin, Jin Tang, and Bin Luo. 2019. Semi-supervised learning with graph learning-convolutional networks. In *Proceedings of the IEEE/CVF conference on computer vision and pattern recognition*. 11313–11320.
- 1394 [14] TN Kipf. 2016. Semi-supervised classification with graph convolutional networks. *arXiv preprint arXiv:1609.02907* (2016).
- 1395 [15] Thomas N. Kipf and Max Welling. 2017. Semi-Supervised Classification with Graph Convolutional Networks. In *International Conference on Learning Representations (ICLR)*.
- 1396 [16] Emirhan Koç, Arda Can Aras, Tuna Alikasifoglu, and Aykut Koç. 2025. Graph-Teacher: Transductive Fine-Tuning of Encoders through Graph Neural Networks. *IEEE Transactions on Artificial Intelligence* (2025).
- 1397 [17] Emirhan Koç, Emre Kulkul, Güleray Kaynar, Tolga Çukur, Murat Acar, and Aykut Koç. 2025. scGraPhT: Merging Transformers and Graph Neural Networks for Single-Cell Annotation. *IEEE Transactions on Signal and Information Processing over Networks* (2025).
- 1398 [18] Ahmed Lamkanfi, Javier Pérez, and Serge Demeyer. 2013. The Eclipse and Mozilla defect tracking dataset: A genuine dataset for mining bug information. In *2013 10th Working Conference on Mining Software Repositories (MSR)*. 203–206. <https://doi.org/10.1109/MSR.2013.6624028>
- 1399 [19] Zhenzhong Lan, Mingda Chen, Sebastian Goodman, Kevin Gimpel, Piyush Sharma, and Radu Soricut. 2020. ALBERT: A Lite BERT for Self-supervised Learning of Language Representations. In *International Conference on Learning Representations (ICLR)*.
- 1400 [20] Sunho Lee. 2023. Duplicate Bug Report Detection by Using Sentence BERT and Faiss. In *Proceedings of the 2nd International Workshop on Intelligent Software Engineering (ISE 2023)*. CEUR-WS.
- 1401 [21] Yinhan Liu, Myle Ott, Naman Goyal, Jingfei Du, Mohit Grover, Ankur Goyal, Omer Tufekci, Smriti Singh, Kanishk Tandon, Vaibhav Khandelwal, et al. 2019. RoBERTa: A Robustly Optimized BERT Pretraining Approach. *arXiv preprint arXiv:1907.11692* (2019).
- 1402 [22] Garima Malik, Mucahit Cevik, and Ayşe Başar. 2023. Data Augmentation for Conflict and Duplicate Detection in Software Engineering Sentence Pairs. In *Proceedings of the ACM Software Engineering Conference*.
- 1403 [23] Christopher D. Manning, Prabhakar Raghavan, and Hinrich Schütze. 2008. *Introduction to Information Retrieval*. Cambridge University Press, Cambridge, UK.
- 1404 [24] Qianru Meng, Xiao Zhang, Guus Ramakers, and Visser Joost. 2024. Combining Retrieval and Classification: Balancing Efficiency and Accuracy in Duplicate Bug Report Detection. *arXiv:2404.14877* [cs.SE]. <https://arxiv.org/abs/2404.14877>
- 1405 [25] Anh Tuan Nguyen, Tung Thanh Nguyen, Tien N. Nguyen, David Lo, and Cheng-nian Sun. 2012. Duplicate bug report detection with a combination of information retrieval and topic modeling. In *Proceedings of the 20th Working Conference on Reverse Engineering (WCRE)*. IEEE, 299–308. <https://doi.org/10.1109/WCRE.2012.38>
- 1406 [26] Lahari Poddar, Leonardo Neves, William Brendel, Luis Marujo, Sergey Tulyakov, and Pradeep Karuturi. 2019. Train One Get One Free: Partially Supervised Neural Network for Bug Report Duplicate Detection and Clustering. *arXiv preprint arXiv:1903.12431* (2019).
- 1407 [27] Nils Reimers and Iryna Gurevych. 2019. Sentence-BERT: Sentence Embeddings using Siamese BERT-Networks. *arXiv preprint arXiv:1908.10084* (2019).
- 1408 [28] Nils Reimers and Iryna Gurevych. 2019. Sentence-BERT: Sentence Embeddings using Siamese BERT-Networks. In *Proceedings of the 2019 Conference on Empirical Methods in Natural Language Processing and the 9th International Joint Conference on Natural Language Processing (EMNLP-IJCNLP)*. Association for Computational Linguistics, Hong Kong, China, 3982–3992. <https://doi.org/10.18653/v1/D19-1410>
- 1409 [29] Gerard Salton and Chris Buckley. 1988. Term-weighting approaches in automatic text retrieval. *Information Processing & Management* 24, 5 (1988), 513–523. [https://doi.org/10.1016/0306-4573\(88\)90021-0](https://doi.org/10.1016/0306-4573(88)90021-0)
- 1410 [30] Victor Sanh, Lysandre Debut, Julien Chaumond, and Thomas Wolf. 2020. DistilBERT, a distilled version of BERT: smaller, faster, cheaper and lighter. *arXiv:1910.01108* [cs.CL]. <https://arxiv.org/abs/1910.01108>
- 1411 [31] Karen Sparck Jones. 1972. A statistical interpretation of term specificity and its application in retrieval. *Journal of Documentation* 28, 1 (1972), 11–21. <https://doi.org/10.1108/eb026526>
- 1412 [32] Chengnian Sun, David Lo, Siau-Cheng Khoo, and Jing Jiang. 2011. Towards more accurate retrieval of duplicate bug reports. In *2011 26th IEEE/ACM International Conference on Automated Software Engineering (ASE)*. IEEE, 253–262. <https://doi.org/10.1109/ASE.2011.6100061>
- 1413 [33] Chengnian Sun, David Lo, Xiaoyin Wang, Jing Jiang, and Siau-Cheng Khoo. 2010. A discriminative model approach for accurate duplicate bug report retrieval. In *Proceedings of the 32nd ACM/IEEE International Conference on Software Engineering (ICSE)*, Vol. 1. ACM, 45–54. <https://doi.org/10.1145/1806799.1806807>
- 1414 [34] Ting Zhang, Amin Khasteh, Minh-Son Le, Hoan Anh Nguyen, and David Lo. 2023. Cupid: Leveraging ChatGPT for More Accurate Duplicate Bug Report Detection. *arXiv:2308.10022* [cs.SE]

Received 16 November 2025

1451
1452
1453
1454
1455
1456
1457
1458
1459
1460
1461
1462
1463
1464
1465
1466
1467
1468
1469
1470
1471
1472
1473
1474
1475
1476
1477
1478
1479
1480
1481
1482
1483
1484
1485
1486
1487
1488
1489
1490
1491
1492
1493
1494
1495
1496
1497
1498
1499
1500
1501
1502
1503
1504
1505
1506
1507
1508